Itinerant ferromagnetism in the As $4p$ conduction band of $Ba_{0.6}K_{0.4}Mn_2As_2$ identified by x-ray magnetic circular dichroism

B. G. Ueland,[1,2,*] Abhishek Pandey,[1,2] Y. Lee,[1,2] A. Sapkota,[1,2] Y. Choi,[3] D. Haskel,[3]
R. A. Rosenberg,[3] J. C. Lang,[3] B. N. Harmon,[1,2] D. C. Johnston,[1,2] A. Kreyssig,[1,2] and A. I. Goldman[1,2]

[1]*Ames Laboratory, U.S. DOE, Iowa State University, Ames, Iowa 50011, USA*
[2]*Department of Physics and Astronomy, Iowa State University, Ames, Iowa 50011, USA*
[3]*Advanced Photon Source, Argonne National Laboratory, Argonne, Illinois 60439, USA*
(Dated: June 1, 2015)

X-ray magnetic circular dichroism (XMCD) measurements on single-crystal and powder samples of $Ba_{0.6}K_{0.4}Mn_2As_2$ show that the ferromagnetism below $T_C \approx 100$ K arises in the As $4p$ conduction band. No XMCD signal is observed at the Mn x-ray absorption edges. Below T_C, however, a clear XMCD signal is found at the As K edge which increases with decreasing temperature. The XMCD signal is absent in data taken with the beam directed parallel to the crystallographic **c** axis indicating that the orbital magnetic moment lies in the basal plane of the tetragonal lattice. These results show that the previously reported itinerant ferromagnetism is associated with the As $4p$ conduction band and that distinct local-moment antiferromagnetism and itinerant ferromagnetism with perpendicular easy axes coexist in this compound at low temperature.

The search for unconventional superconductivity has resulted in the discovery of materials possessing rich, tunable, physical properties and has been the driving force for much recent theoretical and experimental research [1–4]. In particular, the high-temperature cuprate and Fe-pnictide superconductors show remarkable coupling between their lattice, charge, and magnetic degrees of freedom, which may be tuned by small alterations to their chemical structures through, for example, electron- or hole-doping by chemical substitution. [5–7]. These materials have provided testbeds for Hamiltonians based on the Heisenberg model and their applicability to both local-moment and itinerant magnets [2, 8–10]. In particular, the magnetic excitation spectra obtained through inelastic neutron scattering experiments on the parent compounds of the 122-type Fe-pnictide superconductors (AFe_2As_2, $A =$ Ba, Sr, Ca) have been described in terms of the J_1-J_2 Heisenberg model [9, 10].

Systems related to the 122 Fe-pnictides manifest interesting and exotic material properties. For example, $(Ba_{1-x}K_x)(Zn_{1-y}Mn_y)_2As_2$ is a ferromagnetic semiconductor which may be useful for developing multilayer functional devices [11]. The system studied here, $(Ba_{0.6}K_{0.4})Mn_2As_2$, shows local-moment antiferromagnetic (AFM) order below a Néel temperature of $T_N = 480$ K that coexists with half-metallic itinerant ferromagnetic (FM) order below a Curie temperature of $T_C \approx 100$ K [6].

$BaMn_2As_2$ crystallizes in the same body-centered tetragonal $ThCr_2Si_2$ lattice (space group $I4/mmm$) as the parent phases of the superconducting 122 Fe-pnictides [13]. The G-type (checkerboard-type) AFM insulating ground state of the $S = \frac{5}{2}$ Mn spins has an ordered moment of 3.88(4) μ_B/Mn below $T_N = 625(1)$ K that is directed along the **c** axis. [1–4]. It has been demonstrated that $BaMn_2As_2$ can be driven from an insulating to metallic ground state upon the substitution of as little as 1.6% K for Ba [18] or by applied pressure [19]. Nevertheless, $Ba_{1-x}K_xMn_2As_2$ retains the G-type Mn

local-moment AFM order of its parent insulating compound [3, 5, 18]. The AFM order is quite robust, persisting for substitutions up to at least $x = 0.4$ with only nominal changes in T_N and the ordered moment [5]. The partial substitution of K for Ba modifies the electronic structure by hole-doping, and spin-polarized electronic structure calculations and angle-resolved photoemission spectroscopy measurements show that increasing the K doping results in a hole pocket that crosses the Fermi energy [18].

Perhaps most surprising is the observation of a novel ground state in $Ba_{1-x}K_xMn_2As_2$ for $0.16 \leq x \leq 0.4$, where magnetization, nuclear magnetic resonance (NMR), and magnetic field dependent neutron diffraction measurements revealed the onset of itinerant FM below $T_C \approx 100$ K coexisting with the Mn local-moment AFM order [6, 21]. Whereas the moment associated with the AFM order is directed along the unique **c** axis of the tetragonal structure, magnetization data indicate that the FM ordered moments ($\approx 0.45(1)\mu_B$/formula unit for x = 0.4) are aligned perpendicular to this direction, in the **ab** plane [6, 21].

It has been proposed that the FM order in $Ba_{0.6}K_{0.4}Mn_2As_2$ arises from the complete spin polarization of the doped holes in the conduction band (half-metallic ferromagnetism) [6]. Nevertheless, it is reasonable to question whether the observed FM ordering in $Ba_{0.6}K_{0.4}Mn_2As_2$ arises from the canting of the ordered Mn moments. The above mentioned NMR and neutron diffraction measurements argue against this explanation [6], however, recent first-principles calculations suggest that canting of the Mn moments may be induced by a double-exchange interaction [22].

Here, we use the element specificity of x-ray magnetic circular dichroism (XMCD) through measurements on single-crystal and powder samples of $Ba_{0.6}K_{0.4}Mn_2As_2$ to show that FM ordering occurs in the As $4p$ conduction band. We find a strong peak in the XMCD signal at the As K x-ray

absorption edge, but a featureless XMCD signal across the Mn L_2 and L_3 absorption edges. The noise in the signal observed at the Mn L_2 and L_3 absorption edges corresponds to a limit of detection of $0.02 \mu_B$/Mn and is an order of magnitude smaller than the FM moment determined from bulk magnetization measurements [6]. The XMCD signal at the As K edge appears at $T \approx T_C$ due to FM ordering in the As $4p$ conduction band, and its intensity increases with decreasing temperature, in agreement with previous bulk magnetization measurements [6]. Our measurements on single-crystal samples further demonstrate that the FM moments lie in the **ab** plane.

The signal from XMCD measurements is obtained from the differential absorption of circularly-polarized x-rays when the helicity of the incident light is oriented parallel or antiparallel to the magnetization direction of a FM material. During the measurement, the x-ray energy is tuned through the absorption edges of the constituent elements [23–26], providing the elemental specificity. The circularly-polarized photons induce a transition from occupied core states (e.g. $1s$ or $2p$ ground states for K or L edges, respectively) to unoccupied states with energies $E \geq E_F$, where E_F is the Fermi energy. For dipole transitions, changes of $\Delta l = \pm 1$ and $\Delta m_l = \pm 1$ must occur, where l and m_l are the orbital and azimuthal orbital quantum numbers, respectively. Since for K absorption edges the orbital angular momentum is 0 and there is no spin-orbit splitting for the initial state, XMCD probes the magnetic polarization of the orbital moment of the final p states. For L edges, the spin and orbital polarization of the final d states are probed. Hence, XMCD can be viewed as an element- and orbital-specific probe of the magnetization of a sample [27].

Thin ($\sim 100 \mu$m) single crystals of $Ba_{0.6}K_{0.4}Mn_2As_2$ were prepared using the self-flux solution-growth technique described elsewhere [5] and the chemical composition was determined by wavelength-dispersive x-ray spectroscopy [6]. Some single crystals were crushed for measurements on polycrystalline (powder) samples. X-ray absorption spectra (XAS) and XMCD measurements were performed at the Advanced Photon Source at Argonne National Laboratory. Measurements were made across the As and Mn K x-ray absorption edges using station 4-ID-D, and measurements across the Mn L_2 and L_3 absorption edges, using a soft x-ray beam, were accomplished at station 4-ID-C. The single-crystal and powder samples were mounted on Kapton or carbon tape and placed in a He flow cryostat to be cooled down to either $T = 1.8$ K (4-ID-D) or 50 K (4-ID-C). Magnetic fields of $H = 3$ kOe were applied using either a superconducting magnet or an 8-pole electromagnet. This low field value was chosen to saturate the FM signal while minimizing field-induced canting of the Mn moments (see Ref. 6). At both stations, data for circularly-polarized x-rays with helicity parallel [$\mu^+(E)$] and antiparallel to the beam direction [$\mu^-(E)$] were measured to obtain the XMCD signal which is ($\mu^+ - \mu^-$). The XAS signal is proportional to $\frac{1}{2}(\mu^+ + \mu^-)$. To eliminate experimental artifacts, data were taken for both the magnetic field applied parallel and antiparallel to the beam direction. At 4-ID-D,
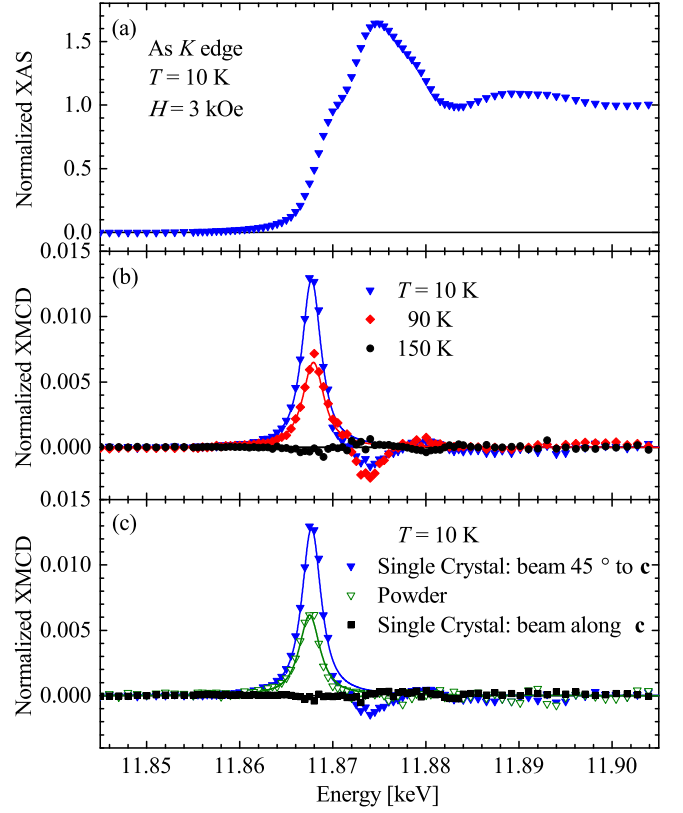

FIG. 1. (Color online) (a) The normalized XAS signal across the As K edge from transmission measurements made on a single-crystal sample. The XAS signal has been normalized to 1 at energies well above the edge. (b) Edge-step normalized XMCD data for $H = 3$ kOe and various temperatures taken with the crystal's **c** axis oriented $45°$ away from the incoming beam ($H_{ab} = 2.1$ kOe). The $T = 10$ K data relate to the XAS data in (a). (c) Edge-step normalized XMCD data for $T = 10$ K and $H = 3$ kOe taken across the As K edge for powder and single-crystal samples. Data for the single crystal are shown for the **c** axis oriented either at $45°$ to the incoming beam or parallel to the beam. The colored lines in (b) and (c) are fits to Lorenztian lineshapes.

a diamond phase retarder was used to circularly polarize the incoming beam, and the x-ray transmission through the samples was measured using an ion chamber detector. Measurements were made using a lock-in technique which alternated the beam's helicity at a frequency of 13.1 Hz [28]. At station 4-ID-C, the circular polarization of the beam was controlled by the undulator, and the total electron yield (TEY) and total fluorescence yield (TFY) were both measured [24].

Figure 1(a) shows the normalized XAS signal across the As K edge for $H = 3$ kOe and Fig. 1(b) shows the corresponding XMCD signal normalized by the absorption edge step. These data were obtained from transmission measurements made on a single crystal with its **c** axis directed $45°$ away from the incoming beam, so that **H** has components along both the **c** axis and basal plane of the tetragonal lattice ($H_c = H_{ab} = 2.1$ kOe). For $T = 10$ K and 90 K, a positive peak is observed just at the absorption threshold. For $T = 90$ K, the
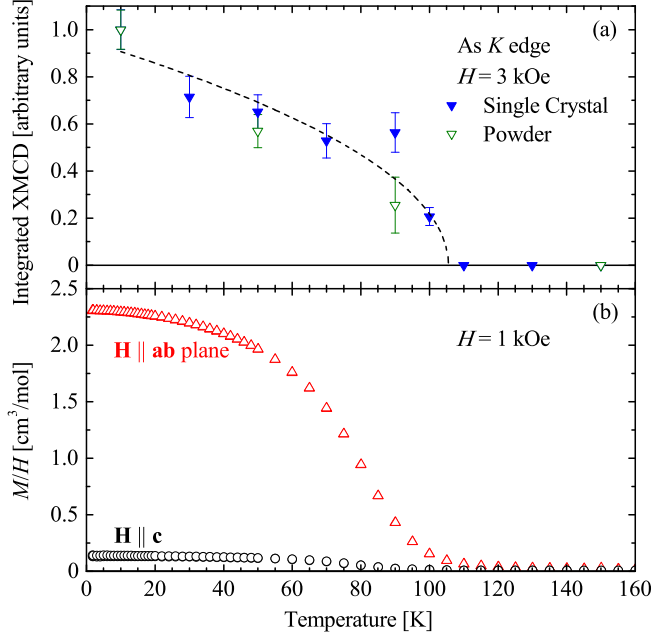
FIG. 2. (Color online) (a) The temperature dependence of the integrated XMCD signal for the $H = 3$ kOe As K edge XMCD data. Data are shown for both a single-crystal sample with its **c** axis oriented 45° away from the incoming beam and a powder sample. The integrated XMCD signal has been determined from fits to the peak in the XMCD data with a Lorentzian lineshape. Both datasets are normalized to their values for $T = 10$ K, and the dashed line is a guide to the eye. (b) $\chi = M/H$ data for $Ba_{0.6}K_{0.4}Mn_2As_2$ from Ref. 6. The nonzero value of χ as $T \to 0$ for **H** applied parallel to the **c** axis is due to a slight misalignment of the crystal ($\approx 4°$) with respect to the field direction [6].

peak has decreased in magnitude and, for $T = 150$ K, the peak is absent. The lines correspond to fits to the peak using a Lorentzian lineshape. These data provide evidence of the FM orbital polarization of the As $4p$ conduction band and are similar in appearance to previous As K edge XMCD spectra in, for example, the $Ga_{1-x}Mn_xAs$ FM semiconductor [29, 30].

The small negative peak observed at a slightly higher incident beam energy arises from linear dichroism contributions due to the incomplete circular polarization of the beam [23]. This is supported by the absence of this negative peak in the data for the powder sample, which are plotted as green open triangles in Fig. 1(c). Figure 1(c) also shows that for $T = 10$ K (below T_C) the positive peak in the XMCD signal is absent with the **c** axis of the sample oriented parallel to the incident x-ray beam (black squares), whereas it is clearly evident for the 45° incident angle (blue triangles) as well as in the powder data. Since XMCD is sensitive to the projection of the sample's magnetization along the beam direction, this demonstrates that the FM moments are perpendicular to **c** and lie within the basal plane.

The As K edge XMCD spectra were recorded at several temperatures between $T = 10$ and 150 K for both the powder and single-crystal samples. The areas determined from
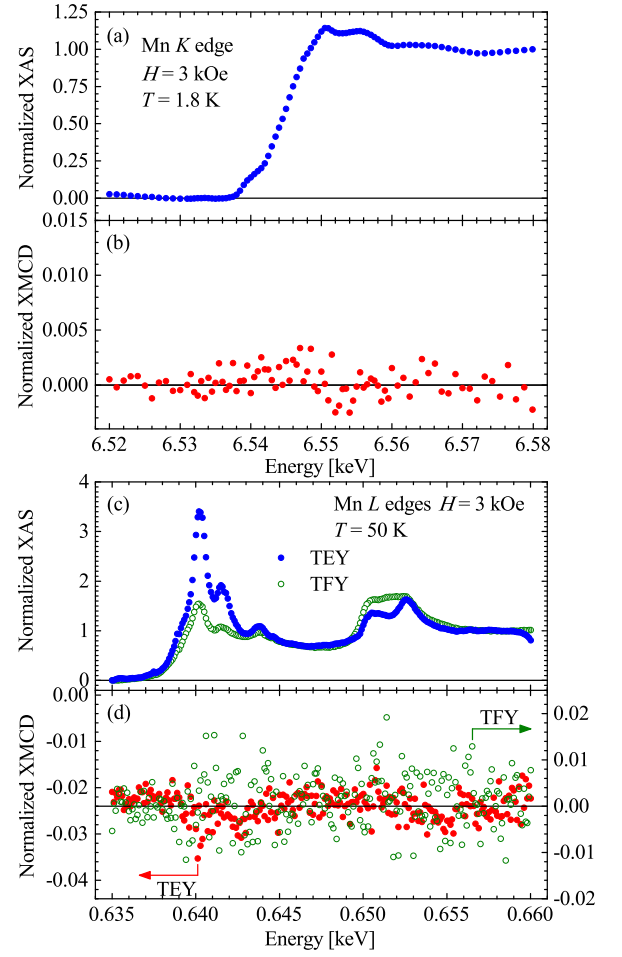

FIG. 3. (Color online) (a) The normalized XAS signal across the Mn K edge for $T = 1.8$ K and $H = 3$ kOe from transmission measurements made on a single-crystal sample with its **c** axis oriented 45° away from the incoming beam. (b) Normalized XMCD data corresponding to the XAS data in (a). (c) Normalized XAS data for $T = 50$ K and $H = 3$ kOe taken across the Mn L_2 and L_3 edges from measurements of the total electron yield (TEY) and total fluorescence yield (TFY) made on a single-crystal sample with its **c** axis oriented 70° away from the incoming beam ($H_{ab} = 2.8$ kOe). (d) Normalized XMCD data corresponding to the TEY (left axis) and TFY (right axis) data in (c). The small constant offset in the TEY data is due to leakage currents and currents induced by external electromagnetic fields in the leads connected to the picoammeter used for the measurements. The TFY data in (c) and (d) have not been corrected for absorption of the fluoresced x-rays by the sample [31].

the fits to the Lorentzian lineshapes are taken as the integrated XMCD signal and are plotted as a function of temperature in Fig. 2(a). Below T_C, the data monotonically increase with decreasing temperature down to the base temperature for our As K edge measurements. Figure 2(b) shows the bulk magnetization data taken from Ref. 6 and demonstrates that the temperature dependence of the integrated XMCD signal for both the single-crystal and powder samples agrees well with the temperature dependence of the bulk magnetization data for **H** parallel to the **ab** plane. The presence of the linear dichro-

ism contamination in the XMCD signal for the single-crystal sample prevents further quantitative analysis of these data.

It is important to consider whether the measured FM can be associated with the Mn moments. To this end, Fig. 3 displays data from XAS and XMCD measurements on single-crystal samples for the Mn K [Figs. 3(a) and 3(b)] and L_2 and L_3 edges [Figs. 3(c) and 3(d)]. For the Mn L_2 and L_3 edge measurements, TEY and TFY data were taken at $T = 50$ K and the sample's $\mathbf{c}$ axis was oriented $70°$ away from the direction of the incident beam ($H_{\mathbf{ab}} = 2.8$ kOe). Measurements at the Mn L_2 and L_3 edges were also made on a powder sample and yielded similar data (not shown). Hence, within the uncertainty of the measurement, we observe no features in the XMCD signals at the Mn K, L_2 and L_3 edges.

Using the normalized XMCD data at the Mn L_2 and L_3 edges from measurements performed on the FM semiconductor $Ga_{0.93}Mn_{0.07}As$ at the same beam-line [32], we can estimate the upper limit for the possible Mn moment within the $\mathbf{ab}$ plane. From Ref. 32, a FM ordered Mn moment of 3 μ_{B} gave rise to a normalized XMCD signal of 2. Applying this proportion to the spread of the noise in our TEY data (which is ~ 0.01), we estimate that our experiments could detect a Mn moment ≥ 0.02 μ_{B}. Performing the same analysis using results from experiments made on $La_{0.7}Sr_{0.3}MnO_3$ ultra-thin films at the European Synchrotron Radiation Facility leads to the same conclusion [33]. Hence, within our experimental sensitivity of 0.02 μ_{B}, we detect no FM contribution from the Mn. This result is also consistent with an upper limit of $M_{\mathbf{ab}} = 0.93(1) \times 10^{-3}$ μ_{B}/Mn due to canting of the AFM Mn moments that we estimate from magnetization data reported in Ref. 6, as described in the Supplemental Material [34]. We note that our TFY data may be strongly distorted by self-absorption effects [31], and we therefore use our TEY data as a basis for the upper estimate of 0.02 μ_{B} for the size of any FM ordered Mn moment present. For measurements at the Mn K edge, comparison to similar data taken for (In,Ga,Mn)As [29] show that our experiments would detect a Mn moment ≥ 0.15 μ_{B}. This indicates that measurements at the Mn L_2 and L_3 edges are an order of magnitude more sensitive to the size of the moment than measurements at the Mn K edge.

Using the normalized XMCD signal obtained for the As K edge, we can determine the value of the orbital moment in the As $4p$ band by applying the sum rule [24, 25, 35]

$$-\frac{\langle L_{\mathrm{z}}\rangle_p}{n_p^{\mathrm{h}}} = \frac{\int_{E_{\mathrm{F}}}^{E_{\mathrm{c}}}(\mu^+ - \mu^-)dE}{P_{\mathrm{c}}\int_{E_{\mathrm{F}}}^{E_{\mathrm{c}}}(\mu^+ + \mu^- + \mu^0)dE}. \quad (1)$$

Here, $\langle L_{\mathrm{z}}\rangle_p$ is the p-projected orbital magnetic moment, n_p^{h} is the number of holes in the p band, $(\mu^+ - \mu^-)$ is equal to the normalized XMCD data, $(\mu^+ + \mu^- + \mu^0)$ is $\frac{3}{2}$ times the normalized XAS data, P_{c} is the degree of circular polarization of the beam, and E_{c} is a cutoff energy above the edge. The contribution to the normalized XAS data from unbound states near E_{F} was modeled by a broadened step function [24] and subtracted before performing the integration in the de-

nominator. Using the $T = 10$ K data for the powder sample, $P_{\mathrm{c}} = 0.95$, which is the nominal degree of circular polarization, and deconvolving the orientational average of the moments in the powder relative to the x-ray beam direction, we find that $\frac{\langle L_{\mathrm{z}}\rangle_p}{n_p^{\mathrm{h}}} = -0.003(1)$ μ_{B}. Taking $n_p^{\mathrm{h}} = 0.2$ holes/As, as done previously [6, 22], we find an As $4p$ orbital moment of $\langle L_{\mathrm{z}}\rangle_p = -0.0006(2)$ μ_{B}/As. The negative sign for $\langle L_{\mathrm{z}}\rangle_p$ implies that the As $4p$ orbital moment is antiparallel to the total moment, which is presumably dominated by the As $4p$ spin moment.

To investigate whether the size of the As $4p$ orbital moment and its direction relative to the spin moment is reasonable in relation to the FM moment of $0.45(1)$ μ_{B}/formula unit determined from magnetization measurements [6], band structure calculations were performed with the Ba atom at the center of the body-centered tetragonal unit cell replaced by a K atom, corresponding to a K doping level of 50%. An artificial magnetic field was added to introduce a spin moment on the As sites, and local spin density approximation calculations were iterated to self-consistency. The converged spin moments on the 2 As sites in the above supercell of the previous primitive cell are 0.24 μ_{B}/As and 0.21 μ_{B}/As, and the orbital moments, induced via the spin-orbit interaction in the As $4p$ band, are both -0.001 μ_{B}/As. The magnitude of the orbital moments as well as their antiparallel orientations to the larger spin moments are in good agreement with the experimental results.

We also note that the value we obtain for the As $4p$ orbital moment is similar to the $4p$ orbital moments calculated for Fe and Ni [36], and to those found from measurements at the As K edge for thin films of the (Ga,Mn)As and (In,Ga,Mn)As FM semiconductors [29, 30]. In these cases, an XMCD signal was also found at the L_2 and L_3 edges of the transition metals, and it was determined that the measured K edge signals were due to polarization of the $4p$ orbital moments by the $3d$ moments of neighboring transition metal sites [29, 30, 36]. As we have shown, this is not the case for $Ba_{0.6}K_{0.4}Mn_2As_2$ since no distinct peaks in the XMCD signal were observed at the Mn edges. Instead, the FM orbital polarization of the As $4p$ states originates from the spin-orbit interaction with spin-polarized As $4p$ states. This assignment is consistent with our previous hypothesis that itinerant FM coexists with the Mn local moment AFM [6].

Summarizing, the presence of an XMCD signal at the As K edge demonstrates that the FM order previously observed in $Ba_{0.6}K_{0.4}Mn_2As_2$ occurs in the As $4p$ conduction band. Our results further show that the FM moments lie in the $\mathbf{ab}$ plane, perpendicular to the AFM ordered Mn moments. Finally, the absence of a net XMCD signal (within the limits of our detection) at the Mn K, L_2, and L_3 edges shows that the FM is not associated with the Mn $3d$ and $4p$ bands, even in light of the substantial Mn-As hybridization evident from electronic structure calculations [2]. These results demonstrate that the local-moment AFM order of the Mn and the itinerant FM in the As $4p$ conduction band are distinct, and illustrate the power of XMCD measurements to assign FM to

a specific element and associated band.

* bgueland@ameslab.gov, bgueland@gmail.com

[1] P. W. Anderson, Science **235**, 1196 (1987).

[2] D. C. Johnston, in *Handbook of Magnetic Materials*, edited by K.H.J. Buschow (Elsevier, Amsterdam, 1997), Vol. 10, pp. 1-237, Chap. 1.

[3] M. B. Maple, E. D. Bauer, V. S. Zapf, and J. Wosnitza, in *Physics of Superconductors*, edited by K. H. Bennemann and J. B. Ketterson (Springer-Verlag, Berlin, 2004), Vol. 2, pp. 555-730.

[4] G. R. Stewart, Rev. Mod. Phys. **83**, 1589 (2011).

[5] J. W. Lynn and P. Dai, Phys. C (Amsterdam, Neth.) **469**, 469 (2009).

[6] J. Paglione and R. L. Greene, Nat. Phys. **6**, 645 (2010).

[7] P. C. Canfield and S. L. Bud'ko, Annu. Rev. Condens. Matter Phys. **1**, 27 (2010).

[8] P.A. Lee, N. Nagaosa, and X.-G. Wen, Rev. Mod. Phys. **78**, 17 (2006).

[9] D. C. Johnston, Adv. Phys. **59**, 803 (2010).

[10] P. Dai, J. Hu, and E. Dagotto, Nat. Phys. **8**, 709 (2012).

[11] K. Zhao, Z. Deng, X. C. Wang, W. Han, J. L. Zhu, X. Li, Q. Q. Liu, R. C. Yu, T. Goko, B. Frandsen, L. Liu, F. Ning, Y. J. Uemura, H. Dabkowska, G. M. Luke, H. Luetkens, E. Morenzoni, S. R. Dunsiger, A. Senyshyn, P. Böni, and C. Q. Jin, Nat. Commun. **4**, 1442 (2013).

[12] A. Pandey, B. G. Ueland, S. Yeninas, A. Kreyssig, A. Sapkota, Y. Zhao, J. S. Helton, J. W. Lynn, R. J. McQueeney, Y. Furukawa, A. I. Goldman, and D. C. Johnston, Phys. Rev. Lett. **111**, 047001 (2013).

[13] E. Brechtel, G. Cordier, and H. Schaefer, Z. Naturforsch. **33b**, 820 (1978).

[14] Y. Singh, A. Ellern, and D. C. Johnston, Phys. Rev. B **79**, 094519 (2009).

[15] J. An, A. S. Sefat, D. J. Singh, and M.-H. Du, Phys. Rev. B **79**, 075120 (2009).

[16] Y. Singh, M. A. Green, Q. Huang, A. Kreyssig, R. J. McQueeney, D. C. Johnston, and A. I. Goldman, Phys. Rev. B **80**, 100403 (2009).

[17] D. C. Johnston, R. J. McQueeney, B. Lake, A. Honecker, M. E. Zhitomirsky, R. Nath, Y. Furukawa, V. P. Antropov, and Y. Singh, Phys. Rev. B **84**, 094445 (2011).

[18] A. Pandey, R. S. Dhaka, J. Lamsal, Y. Lee, V. K. Anand, A. Kreyssig, T. W. Heitmann, R. J. McQueeney, A. I. Goldman, B. N. Harmon, A. Kaminski, and D. C. Johnston, Phys. Rev. Lett. **108**, 087005 (2012).

[19] A. T. Satya, A. Mani, A. Arulraj, N. V. Chandra Shekar, K. Vinod, C. S. Sundar, and A. Bharathi, Phys. Rev. B **84**, 180515(R) (2011); **85**, 019901(E) (2012).

[20] J. Lamsal, G. S. Tucker, T. W. Heitmann, A. Kreyssig, A. Jesche, A. Pandey, W. Tian, R. J. McQueeney, D. C. Johnston, and A. I. Goldman, Phys. Rev. B **87**, 144418 (2013).

[21] J.-K. Bao, H. Jiang, Y.-L. Sun, W.-H. Jiao, C.-Y. Shen, H.-J. Guo, Y. Chen, C.-M. Feng, H.-Q. Yuan, Z.-A. Xu, G.-H. Cao, R. Sasaki, T. Tanaka, K. Matsubayashi, and Y. Uwatoko, Phys. Rev. B **85**, 144523 (2012).

[22] J. K. Glasbrenner and I. I. Mazin, Phys. Rev. B **89**, 060403(R) (2014).

[23] S. W. Lovesey and S. P. Collins, *X-Ray Scattering and Absorption by Magnetic Materials* (Oxford University Press, Oxford, 1996).

[24] J. C. Lang, in *Characterization of Materials*, edited by E. N. Kaufmann (John Wiley & Sons, New York, 2003), Second Edition.

[25] B. T. Thole, Paolo Carra, F. Sette, and G. van der Laan, Phys. Rev. Lett. **68**, 1943 (1992).

[26] P. Carra, B. T. Thole, M. Altarelli, and X. Wang, Phys. Rev. Lett. **70**, 694 (1993).

[27] For an example see: D. Haskel, J. C. Lang, Z. Islam, A. Cady, G. Srajer, M. van Veenendaal, and P. C. Canfield, Phys. Rev. Lett. **95**, 217207 (2005).

[28] M. Suzuki, N. Kawamura, M. Mizumaki, A. Urata, H. Maruyama, S. Goto, and T. Ishikawa, Jpn. J. Appl. Phys. **37**, L1488 (1998).

[29] A. A. Freeman, K. W. Edmonds, G. van der Laan, R. P. Campion, A. W. Rushforth, N. R. S. Farley, T. K. Johal, C. T. Foxon, B. L. Gallagher, A. Rogalev, and F. Wilhelm, Phys. Rev. B **77**, 073304 (2008).

[30] P. Wadley, A. A. Freeman, K. W. Edmonds, G. van der Laan, J. S. Chauhan, R. P. Campion, A. W. Rushforth, B. L. Gallagher, C. T. Foxon, F. Wilhelm, A. G. Smekhova, and A. Rogalev, Phys. Rev. B **81**, 235208 (2010).

[31] Attempts to correct the TFY data for self-absorption effects using two different methods were unsuccessful.

[32] D. J. Keavney, D. Wu, J. W. Freeland, E. Johnston-Halperin, D. D. Awschalom, and J. Shi, Phys. Rev. Lett. **91**, 187203 (2003).

[33] C. Aruta, G. Ghiringhelli, V. Bisogni, L. Braicovich, N. B. Brookes, A. Tebano, and G. Balestrino, Phys. Rev. B **80**, 014431 (2009).

[34] See Supplemental Material at [URL will be inserted by publisher] for a discussion of the expected canting of the Mn moments away from the **c** axis by the applied magnetic field.

[35] G. Y. Guo, J. Phys.: Condens. Matter **8**, L747 (1996).

[36] J. I. Igarashi and K. Hirai, Phys. Rev. B **50**, 17820 (1994).

Supplemental Materials:
Itinerant ferromagnetism in the As $4p$ conduction band of $Ba_{0.6}K_{0.4}Mn_2As_2$ identified by x-ray magnetic circular dichroism
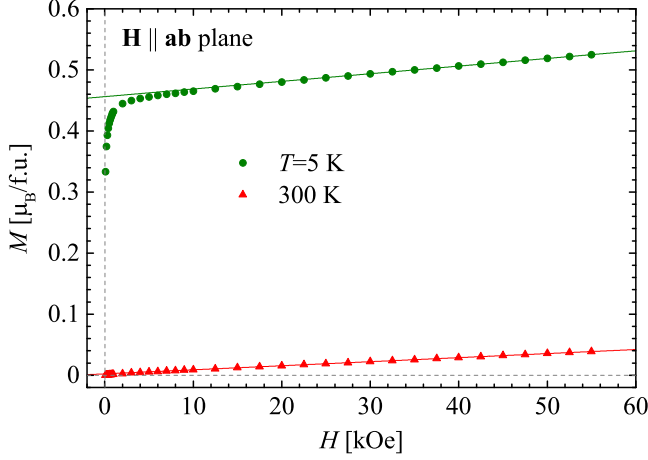

FIG. S1. (Color online) Magnetization versus field data for a single crystal sample at various temperatures, taken from Ref. S6 . The field was applied along the **ab** plane. f.u. stands for formula unit. Lines are linear fits between $H = 30$ and 55 kOe.

Since local-moment G-type antiferromagnetic (AFM) order of the Mn sublattice exists below $T_N = 480$ K with an ordered moment of $3.88(4)$ μ_B/Mn that lies along the **c** axis of the tetragonal unit cell [S1–S5], it is important to consider how the magnetic field applied in the **ab** plane for the XMCD measurements would cant the ordered Mn moments away from the **c** axis. Below, we set an upper limit of $0.93(1) \times 10^{-3}$ μ_B/Mn for the magnetization in the **ab** plane that would occur due to canting of the AFM ordered Mn moments by a field of $H = 2.8$ kOe. This value is well below the estimated detection limit of 0.02 μ_B for our XMCD measurements at the Mn L_2 and L_3 edges.

EXPECTED CANTING OF THE Mn MOMENTS BY THE APPLIED MAGNETIC FIELD

Previous results for insulating $BaMn_2As_2$ have shown that fits to the high-field range of magnetization versus field data accurately determine the magnetic susceptibility of the AFM ordered Mn sublattice [S1]. Hence, we expect that similar fits to data for metallic $Ba_{0.6}K_{0.4}Mn_2As_2$ may be used to estimate the susceptibility of the ordered Mn sublattice, provided that we consider data for either $T \ll T_C$ or $T_C \ll T \ll T_N$.

Figure S1 shows magnetization M versus field data from measurements made on a single-crystal sample with **H** applied along the **ab** plane after cooling in zero field. The $T = 5$ K data illustrate the dramatic rise in M at low fields due to the itinerant FM order. Above $H \approx 2$ kOe the contribution due to the itinerant FM order approaches saturation, and for $H \geq 30$ kOe M is a linear function of H up to at least 55 kOe.

By fitting the $T = 5$ K data between $H = 30$ and 55 kOe to a line, we find a slope of $\chi_{ab} = \frac{dM_{ab}}{dH} = 1.25(1) \times 10^{-3}$ μ_B/kOe-f.u. Multiplying this value by 2.8 kOe (the magnitude of the applied field in the **ab** plane during the Mn L_2 and L_3 edge XMCD experiments), and by assuming that the field-induced magnetization for $H \geq 30$ kOe comes entirely from the Mn moments, we obtain an upper limit of $M_{ab} = 1.75(1) \times 10^{-3}$ μ_B/Mn. Applying the same procedure to the 300 K data (i.e. data for $T_C << T << T_N$), we obtain a slope of $\chi_{ab} = 0.66(1) \times 10^{-3}$ μ_B/kOe-f.u. and a magnetization of $M_{ab} = 0.93(1) \times 10^{-3}$ μ_B/Mn. Since the doped-hole FM may not be completed saturated at $H = 3$ kOe, and χ_{ab} is likely somewhat temperature dependent, the discrepancy between the values of M_{ab} for $T = 5$ and 300 K appears reasonable. In any case, both of the values are far below the detection limit of ≈ 0.02 μ_B for our XMCD experiments at the Mn L_2 and L_3 edges.

* bgueland@ameslab.gov, bgueland@gmail.com
[S1] Y. Singh, A. Ellern, and D. C. Johnston, Phys. Rev. B **79**, 094519 (2009).
[S2] J. An, A. S. Sefat, D. J. Singh, and M.-H. Du, Phys. Rev. B **79**, 075120 (2009).
[S3] Y. Singh, M. A. Green, Q. Huang, A. Kreyssig, R. J. Mc-Queeney, D. C. Johnston, and A. I. Goldman, Phys. Rev. B **80**, 100403 (2009).
[S4] D. C. Johnston, R. J. McQueeney, B. Lake, A. Honecker, M. E. Zhitomirsky, R. Nath, Y. Furukawa, V. P. Antropov, and Y. Singh, Phys. Rev. B **84**, 094445 (2011).
[S5] J. Lamsal, G. S. Tucker, T. W. Heitmann, A. Kreyssig, A. Jesche, A. Pandey, W. Tian, R. J. McQueeney, D. C. Johnston, and A. I. Goldman, Phys. Rev. B **87**, 144418 (2013).
[S6] A. Pandey, B. G. Ueland, S. Yeninas, A. Kreyssig, A. Sapkota, Y. Zhao, J. S. Helton, J. W. Lynn, R. J. McQueeney, Y. Furukawa, A. I. Goldman, and D. C. Johnston, Phys. Rev. Lett. **111**, 047001 (2013).